

# The DNA-Dependent Protein Kinase Interacts with DNA To Form a Protein–DNA Complex That Is Disrupted by Phosphorylation<sup>†</sup>

Dennis Merkle,<sup>‡,§,||,⊥</sup> Pauline Douglas,<sup>‡,§,⊥</sup> Greg B. G. Moorhead,<sup>§</sup> Zoya Leonenko,<sup>||</sup> Yaping Yu,<sup>‡,§</sup> David Cramb,<sup>||</sup> David P. Bazett-Jones,<sup>#</sup> and Susan P. Lees-Miller<sup>\*,‡,§</sup>

Department of Biochemistry & Molecular Biology, University of Calgary, 3300 Hospital Drive, Calgary AB, T2N 4N1, Canada, Departments of Biological Sciences and of Chemistry, University of Calgary, 2500 University Drive, N.W., Calgary AB, T2N 1N4, Canada, and Program in Cell Biology, Research Institute, The Hospital for Sick Children, 555 University Avenue, Toronto, Ontario M5G 1X8, Canada

Received June 26, 2002; Revised Manuscript Received August 16, 2002

**ABSTRACT:** DNA double-strand breaks are a serious threat to genome stability and cell viability. One of the major pathways for the repair of DNA double-strand breaks in human cells is nonhomologous end-joining. Biochemical and genetic studies have shown that the DNA-dependent protein kinase (DNA-PK), XRCC4, DNA ligase IV, and Artemis are essential components of the nonhomologous end-joining pathway. DNA-PK is composed of a large catalytic subunit, DNA-PKcs, and a heterodimer of Ku70 and Ku80 subunits. Current models predict that the Ku heterodimer binds to ends of double-stranded DNA, then recruits DNA-PKcs to form the active protein kinase complex. XRCC4 and DNA ligase IV are subsequently required for ligation of the DNA ends. Magnesium-ATP and the protein kinase activity of DNA-PKcs are essential for DNA double-strand break repair. However, little is known about the physiological targets of DNA-PK. We have previously shown that DNA-PKcs and Ku undergo autophosphorylation, and that this correlates with loss of protein kinase activity. Here we show, using electron spectroscopic imaging, that DNA-PKcs and Ku interact with multiple DNA molecules to form large protein–DNA complexes that converge at the base of multiple DNA loops. The number of large protein complexes and the amount of DNA associated with them were dramatically reduced under conditions that promote phosphorylation of DNA-PK. Moreover, treatment of autophosphorylated DNA-PK with the protein phosphatase 1 catalytic subunit restored complex formation. We propose that autophosphorylation of DNA-PK plays an important regulatory role in DNA double-strand break repair by regulating the assembly and disassembly of the DNA-PK–DNA complex.

DNA double-strand breaks (DSBs)<sup>1</sup> occur naturally as a result of oxidative metabolism, V(D)J recombination, and stalled replication forks, and can also be introduced by exogenous sources, such as ionizing radiation and radiomi-

metic drugs. In human cells, DNA DSBs are repaired by one of two pathways, namely, homologous recombination or nonhomologous end-joining (NHEJ) [reviewed in (1, 2)]. The first step in NHEJ is thought to be assembly of the DNA-dependent protein kinase, DNA-PK, at the site of the DNA DSB. DNA-PK is composed of a 469 kDa catalytic subunit, DNA-PKcs, and a heterodimer of 70 and 83 kDa subunits (Ku70/80) [reviewed in (3)]. In *in vitro* assays, Ku binds to ends of double-stranded (ds) DNA with high affinity (4), and has the ability to translocate along naked DNA in an ATP-independent manner (5). DNA-PKcs interacts with ends of linear dsDNA (6, 7), but has weak protein kinase activity in the absence of Ku (8–10). Current models predict that Ku binds to ends of dsDNA, translocates inward, and then recruits DNA-PKcs to form the active DNA-PK complex [reviewed in (1, 3)]. XRCC4 and DNA ligase IV are also required for NHEJ, and are presumably recruited to the DNA DSB site, where they act to ligate the DNA ends.

DNA-PK-dependent end-joining in cell-free extracts from human cells requires Mg-ATP and is inhibited by the fungal metabolite wortmannin (11–13). Wortmannin inhibits the protein kinase activity of DNA-PK and other phosphatidylinositol 3-kinase related proteins at nanomolar concentrations *in vitro* (14–16), radiosensitizes cells, and inhibits DNA

<sup>†</sup> This work was funded through a Pilot Project grant from the Alberta Cancer Foundation (to S.P.L.-M. and D.C.), Grant 13639 from the Canadian Institutes of Health Research (to S.P.L.-M.), and operating grants from the Natural Sciences and Engineering Research Council to D.P.B.-J. and G.B.G.M. S.P.L.-M. is a Heritage Medical Scientist of the Alberta Heritage Foundation for Medical Research. P.D. is a Postdoctoral Fellow of the Alberta Heritage Foundation for Medical Research. D.P.B.-J. holds a Canada Research Chair in Molecular and Cellular Imaging.

\* Correspondence should be addressed to this author at the Department of Biochemistry and Molecular Biology, 145 Biosciences Building, University of Calgary, 2500 University Dr., NW, Calgary, AB, T2N 1N4, Canada. Phone: (403) 220-7628; Fax: (403) 289-9311; Email: leesmill@ucalgary.ca.

<sup>‡</sup> Department of Biochemistry & Molecular Biology, University of Calgary.

<sup>§</sup> Department of Biological Sciences, University of Calgary.

<sup>||</sup> Department of Chemistry, University of Calgary.

<sup>⊥</sup> The first two authors contributed equally to this work.

<sup>#</sup> Program in Cell Biology, The Hospital for Sick Children.

<sup>1</sup> Abbreviations: AFM, atomic force microscopy; bp, base pair(s); DNA-PK, DNA-dependent protein kinase; DNA-PKcs, DNA-dependent protein kinase catalytic subunit; DSB, double-strand break; ds, double-stranded; ESI, electron spectroscopic imaging; MC-LR, microcystin-LR; NHEJ, nonhomologous end-joining; PP1, protein phosphatase 1.

DSB repair in vivo (17, 18). DNA-PK kinase activity is also essential in vivo, as complementation of DNA-PKcs-defective cells with wild-type DNA-PKcs, but not with DNA-PKcs containing mutations in the kinase domain, restores the wild-type phenotype (19). Together, these studies indicate that the protein kinase activity of DNA-PK is essential for its biological function.

DNA-PK phosphorylates a number of substrates in vitro (3); however, its physiological targets in nonhomologous end-joining are unknown. We have shown that DNA-PK phosphorylates itself in vitro on all three subunits, DNA-PKcs, Ku70, and Ku80. Autophosphorylation of DNA-PK correlates with loss of protein kinase activity (20, 21), and protein phosphatases reverse this phosphorylation-induced loss of activity (22). We, therefore, propose a model in which DNA-PK is less active in its hyper-phosphorylated state and more active in its hypo-phosphorylated state. We have shown, using purified proteins, that DNA-PKcs and Ku only co-immunoprecipitate in the presence of DNA, and that preincubation of DNA-PKcs and Ku with DNA in the presence of Mg-ATP prevents this interaction (21), suggesting that autophosphorylation results in dissociation of the DNA-PK complex. In Southwestern assays, the phosphorylated Ku70 polypeptide retained its ability to bind to DNA, indicating that the phosphorylated Ku 70/80 heterodimer may also interact with DNA after dissociation of phosphorylated DNA-PKcs (21). From these experiments, we suggest that dissociation of phosphorylated DNA-PKcs from phosphorylated, DNA-bound Ku could account for the phosphorylation-induced loss of DNA-PK protein kinase activity.

Interaction between the Ku70/80 heterodimer and linear dsDNA has been observed using electron microscopy (5) and atomic force microscopy (AFM) (6, 7, 23). AFM studies show that the Ku heterodimer binds to ends and internal sites in linear dsDNA, and that Ku-DNA complexes can form loop or lariat structures (6, 7). In contrast, DNA-PKcs binds predominantly to the ends of dsDNA (6, 7). Here, we have used energy-filtered transmission electron microscopy or electron spectroscopic imaging (ESI) to study the interaction of highly purified DNA-PKcs and Ku with dsDNA. ESI is based on the principle of electron energy loss spectroscopy, and yields high-contrast images without the requirement for resolution-limiting, heavy-atom contrast agents (24–26). Also, ESI allows us to distinguish between molecules containing a high percentage of phosphorus (such as DNA), and proteins (24–26). Using ESI, we provide direct physical evidence that DNA-PKcs and Ku interact with DNA ends to form a large protein-DNA complex and that this complex is located at the convergence of multiple DNA loops. Moreover, we show that incubation with Mg-ATP largely abolishes the large protein complexes, while treatment with protein phosphatase leads to their restoration, suggesting that formation of these complexes is a dynamic, reversible process.

## MATERIALS AND METHODS

**Reagents.** Wortmannin (Sigma Chemical Co.) stock solution was made up at 10 mM in DMSO, and diluted 500-fold in water (Tissue Culture Grade, Life Technologies) immediately before use. For untreated controls, an equivalent volume of DMSO was diluted 500-fold in water and added

to the reactions. Microcystin-LR was purchased from Calbiochem. PHAS-I was obtained from Stratagene.

**DNA.** pGEM7Zf(+) plasmid DNA (Promega) was purified from *E. coli* JM109 using a QIAGEN plasmid Midi Kit according to the manufacturer's instructions. The purity and integrity of the resulting closed circular DNA was monitored by electrophoresis on 0.8% agarose gels, and the concentration of DNA was quantitated by absorbance at 260 nm. Closed circular DNA was linearized by incubation with *EcoRI* (5' 4 bp overhanging ends), *SphI* (3' 4 bp overhanging ends), or *SmaI* (blunt ends) at 37 °C for 1 h. Efficiency of linearization was confirmed by agarose gel electrophoresis, and, in all cases, was estimated to be greater than 95%. The restriction enzyme was heat-inactivated by incubation at 75 °C for 5 min, and the linearized DNA was extracted once with phenol/chloroform (1:1), followed by ethanol precipitation. The DNA was stored at –20 °C in 10 mM Tris-HCl, pH 8.0, 1 mM EDTA, and diluted to 0.4 mg/mL in 10 mM Tris-HCl, pH 8.0, before use.

**Proteins.** DNA-PKcs and Ku were purified from human placenta to at least 98% homogeneity as described previously (10). The reconstituted DNA-PK enzyme (DNA-PKcs plus Ku) was highly active with a specific activity of 800–1000 units/mg toward the peptide substrate PESQEAFADLWKK (1 unit is defined as the amount of protein required to transfer 1 nmol of phosphate per minute). Procedures for purification of recombinant protein phosphatase 1 (PP1), DNA-PK activity assays, and immunoprecipitation were as described previously (22).

**Preparation of Samples for Microscopy.** Purified Ku heterodimer was incubated alone, or in the presence of DNA-PKcs, with 100 ng of linearized DNA in buffer containing 25 mM Hepes, pH 7.9, and 50 mM KCl, in a final volume of 10  $\mu$ L. Samples were centrifuged for 30 s at approximately 14000g in a refrigerated microcentrifuge, and then placed on ice for 30 min. Immediately prior to microscopy, samples were diluted 10-fold in ESI buffer (25 mM Hepes, pH 7.9, 50 mM KCl, 5 mM MgCl<sub>2</sub>). All solutions for ESI were prepared in tissue culture grade water (Life Technologies, Inc.).

For autophosphorylation reactions, proteins were incubated with 5 mM MgCl<sub>2</sub> and 0.5 mM ATP (or 0.5 mM AMP-PNP) at 30 °C for 1 h before being placed on ice and diluted in ESI buffer. Where indicated, wortmannin (1  $\mu$ M final concentration) was added to reactions containing DNA-PKcs, Ku, and DNA 10 min prior to addition of ATP. Where indicated, after the autophosphorylation reaction, recombinant PP1 catalytic subunit was added to 40 milliunits/mL (1 unit is defined as the amount of protein phosphatase required to release 1  $\mu$ mol of phosphate from phosphorylase *a* per minute under standard assay conditions). Samples were then incubated at 30 °C for an additional 10 min before dilution in ESI buffer and microscopy as above. For control reactions, microcystin-LR (1  $\mu$ M) was added to PP1 catalytic subunit for 5 min at room temperature prior to addition to autophosphorylation reactions.

**Microscopy.** Carbon-coated copper grids were prepared as previously described (24). Five microliters of diluted sample was applied at room temperature to 1000-mesh, carbon-coated copper grids. After 1 min, grids were carefully washed of excess sample by gently swiping through water (Tissue Culture Grade, Life Technologies), containing 1 drop

of "PhotoFlow" detergent (Kodak) per 20 mL of water. Grids were then gently blotted dry with filter paper, and allowed to air-dry for 1 min.

Samples were analyzed using an EM902 energy-filtering transmission electron microscope with an in-column prism-mirror-prism spectrometer (LEO, Oberkochen, Germany), equipped with a 12-bit, cooled CCD detector (Gatan, Pleasanton, CA). Images were recorded at 85000 $\times$  magnification with energy losses at 155 eV (for phosphorus post-ionization edge imaging) and 120 eV (for mass specific imaging). Exposure times for the 155 and 120 eV images were 35 and 17 s, respectively.

**Image Analysis.** For sample analysis, a random selection of DNA–protein molecules on the grid was examined and scored for the type of protein–DNA complex observed. Between 10 and 100 samples were scored for each experiment. Each experiment was repeated at least 3 times, and results are representative of each experiment.

To produce net phosphorus specific images, the sum of four equivalent 155 eV images was divided by the sum of four equivalent 120 eV images using image analysis software (ErgoVista, Ottawa). To map the DNA within the protein complexes, the 120 eV mass-sensitive image was false-colored green and overlaid on a false-colored red net phosphorus image using Adobe Photoshop. Mass images were false-colored green, while all net phosphorus images were false-colored red. The dimensions of the protein complexes were determined by performing a line scan of the intensity of the 120 eV image complexes using Image-J software (NIH). One pixel equals 1.42 nm at 85000 $\times$  magnification. Scale bars represent 100 nm.

## RESULTS

### *Characterization of Protein–DNA Complexes Using ESI.*

The length of a single linearized plasmid dsDNA molecule (3000 bp), as measured in ESI, was approximately 1022 nm (Figure 1A). As has been observed previously (6, 7, 23), when linearized dsDNA was preincubated with purified Ku70/80 heterodimer, Ku molecules were observed at ends and internal sites of the dsDNA (Figure 1B, arrows). Approximately 80% of the Ku molecules were internally bound, with the remaining 20% of the molecules bound at DNA ends. Approximately 80–87% of the DNA molecules were in a linear conformation, with 13–20% assuming loop or lariat conformations (Table 1). The size of the individual DNA-bound Ku molecules was estimated as 13.4 nm (range = 11.1–14.8 nm,  $n = 11$ ) for the shorter axis, and 14.8 nm (range = 13.4–16.2 nm,  $n = 11$ ) for the longer axis. When increasing amounts of Ku heterodimer (3–12 nM) were titrated into constant amounts of linear dsDNA (5 nM), the proportion of straight versus looped DNA was not significantly altered. When Ku was present at 3 nM, the average number of Ku molecules per DNA molecule was approximately 1 (1.2 per DNA molecule,  $n = 55$ ), whereas at higher concentrations of Ku (6–13 nM), an average of 6 molecules of Ku were observed per DNA molecule ( $n = 20$ ) (Table 1). These data are consistent with previous studies showing concentration-dependent loading of Ku onto linear dsDNA (5, 27).

We and others have shown that purified DNA-PKcs has weak DNA-dependent protein kinase activity compared to

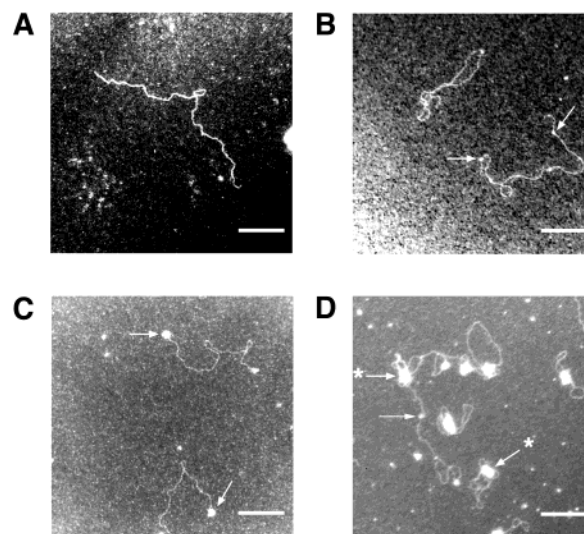


**FIGURE 1:** ESI images of linearized plasmid DNA incubated without or with purified Ku70/80 heterodimer and DNA-PKcs. Samples were prepared for microscopy as described under Materials and Methods. Panel A: linear plasmid dsDNA. Panel B: 5 ng (0.16 pmol) of purified Ku70/80 heterodimer was incubated with 100 ng of linearized plasmid dsDNA (final volume 10  $\mu$ L), and then analyzed by microscopy as described. The arrow indicates an example of DNA-bound Ku. Panel C: 15 ng of purified DNA-PKcs (0.16 pmol) was incubated with 100 ng of DNA in the absence of Ku70/80 and then analyzed as described. The arrow indicates DNA-bound DNA-PKcs. Panel D: DNA-PKcs (15 ng) was incubated with Ku70/80 (5 ng) and linear dsDNA and prepared for ESI as indicated above. A Ku–DNA complex is indicated by the arrow. The possible interaction of two large protein complexes (formed in the presence of DNA-PKcs and Ku) is indicated by the arrow with an asterisk. The scale bar represents 100 nm.

that of DNA-PKcs plus the Ku heterodimer (8–10). We previously reported that highly purified DNA-PKcs did not bind to short deoxyoligonucleotides under conditions of electrophoretic mobility shift assays (28). However, binding of DNA-PKcs to ends of longer fragments of linear dsDNA has been observed using AFM (6, 7). When samples containing DNA-PKcs and DNA were analyzed by ESI, approximately 20% of the DNA molecules contained DNA-PKcs. Over 80% of the DNA molecules existed in an extended form with no DNA-PKcs bound. In the cases where DNA-PKcs was bound to DNA, it was only detected at DNA ends, and the DNA was linear; i.e., no looping or lariat formation was observed (Table 3 and Figure 1C, end bound DNA-PKcs indicated by the arrows). The DNA-PKcs molecule was roughly spherical with an average long axis of 28.7 nm (range = 18.5–27.0 nm,  $n = 6$ ) and an average short axis of 24.2 nm (range = 25.6–32.7 nm,  $n = 6$ ). Titration of increasing amounts of DNA-PKcs to linear dsDNA did not induce a significant increase in the amount of DNA-PKcs bound to the DNA ends (data not shown). The images shown in Figure 1 contain plasmid dsDNA that was linearized with *EcoRI* to contain 4 bp overhanging ends. No significant differences in either the type of protein–DNA complexes observed or the proportion of protein–DNA to free DNA were observed when dsDNA was linearized with *SphI*, to create 3' ends with a 4 bp overhang, or *SmaI*, to create blunt ends (Table 2). Unless otherwise indicated, all subsequent images were obtained with *EcoRI* linearized DNA.

Table 1: Interaction of Ku70/80 Heterodimer with Linear dsDNA<sup>a</sup>

concn of Ku in assays (nM)	no. of Ku molecules bound at internal DNA sites	no. of Ku molecules bound to ends of DNA	average no. of Ku molecules per DNA molecule	range of total no. of Ku molecules bound to DNA	no. of DNA molecules present in loop or lariat formation	<i>n</i>
3	52 (79%)	14 (21%)	1.2	0–11	7 (13%)	55
6	93 (84%)	18 (16%)	5.6	1–10	4 (20%)	20
12	94 (83%)	19 (17%)	5.7	2–10	3 (15%)	20

<sup>a</sup> Ku70/80 was incubated with linear dsDNA (5 nM) at the concentrations shown. *n* indicates the number of single linear dsDNA molecules analyzed in each experiment. The number of complexes observed relative to the total number of DNA molecules analyzed is shown in parentheses.

Table 2: Interaction of DNA-PKcs with Differing DNA Ends<sup>a</sup>

type of DNA end	no. of DNA-PKcs complexes	no. of DNA-PKcs per DNA	range of DNA-PKcs per DNA	<i>n</i>
5' 4 bp overhangs	6	0.17	0–1	35
3' 4 bp overhangs	4	0.11	0–2	35
blunt	4	0.11	0–2	35

<sup>a</sup> DNA-PK was incubated with 5 nM linear DNA of various forms (as indicated). The concentration of DNA in each sample was 5 nM, and DNA-PKcs was present at 3 nM. The complexes formed were only present at the DNA ends. *n* indicates a single DNA molecule.

Incubation of DNA-PKcs and Ku with DNA resulted in a dramatic difference in the appearance of the DNA and the protein–DNA complexes (Figure 1D). Rather than appearing as linear molecules, the DNA molecules contained large loops that were associated with large protein complexes. In most cases, several DNA molecules were associated with each large protein complex. Free ends of DNA were not found protruding from these large complexes, suggesting that they are enclosed within the protein complex. Together, these observations suggest that the DNA-PKcs–Ku complex interacts with the ends of multiple DNA molecules, and sequesters them in the large protein–DNA complex. The protein complexes were roughly spherically shaped with an average longer axis of 40.0 nm (range = 29.8–58.2 nm, *n* = 6) and a shorter axis of 36.2 nm (range = 25.6–56.8 nm, *n* = 6) (Figure 1D, indicated by the arrow). These protein complexes were visibly larger than those formed by Ku or DNA-PKcs alone. In some cases, two protein complexes appeared to interact to form a larger complex (Figure 1D, indicated by arrow marked with an asterisk). Similar results were observed over a range of concentrations of DNA-PKcs and Ku (between 3 and 12 nM), and with DNA with 3'-overhanging or blunt ends. Approximately 50–90% of the large protein complexes were associated with multiple DNA molecules, with an average of approximately 1.2 protein complexes per DNA population.

*DNA-PK Complexes Are Located at the Convergence of Multiple DNA Loops.* One feature of ESI is the ability to distinguish between proteins and molecules that contain high levels of phosphorus, such as nucleic acids (24, 26, 29). We therefore used this feature to track the path of DNA through the large protein–DNA complexes. Net phosphorus images were produced of DNA-PKcs plus DNA in the absence and presence of Ku. By overlaying the net phosphorus image (colored red in Figure 2, panels B and E) on the 120 eV mass image (colored green in Figure 2, panels A and D), the path of the DNA was followed through the protein complex (Figure 2, panels C and F). In the absence of Ku, DNA-PKcs was present at the end of the DNA molecule (Figure 2A). When both Ku and DNA-PKcs were present,

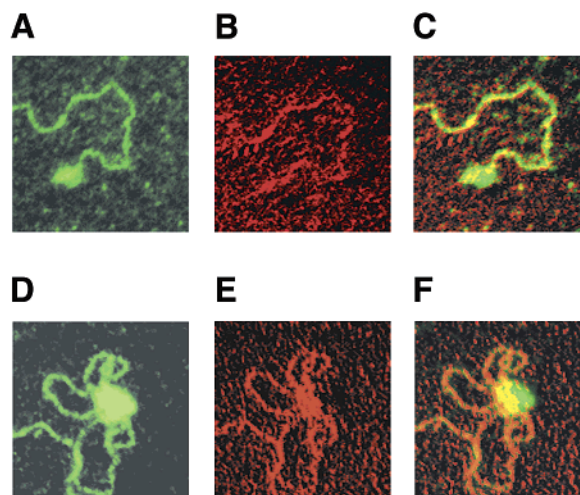


FIGURE 2: Interaction of linear plasmid dsDNA with DNA-PKcs in the absence and presence of the Ku heterodimer: Linear plasmid dsDNA was incubated with DNA-PKcs in the absence or presence of Ku and prepared for ESI as described under Materials and Methods. Panels A–C were obtained from incubation of DNA-PKcs plus DNA and are of a single molecule of DNA-PKcs bound to the end of the DNA molecule. Panel A: The 120 eV image (representing the mass of the DNA and the protein), false-colored green. Panel B: The net phosphorus image of the 120 eV image shown in panel A. This panel represents only the DNA content of the image and is false-colored red. Panel C: Overlay of the images in panels A and B. The yellow color corresponds to areas of overlap between the DNA content (red) and the total mass (green) of the protein complex. Panels D–F were obtained from reactions containing DNA-PKcs plus Ku and DNA. A single large protein complex interacting with multiple DNA molecules is shown. Panel D: The 120 eV image, representing both the mass of the protein and the DNA, false-colored green. Panel E: The net phosphorus image of the 120 eV image shown in panel D. This panel represents only the DNA content of the image and is false-colored red. Panel F: Overlay of the images in panels D and E. The yellow color corresponds to the areas of overlap between the DNA content (red) and the total mass (green) of the complex.

the DNA was highly convoluted in appearance, with several loops emanating from a central region of DNA (Figure 2D–F). The protein complex (shown in green in Figure 2F) was located over the convergence of the DNA loops. The yellow area of the protein molecule(s) represents the total mass (i.e., protein + DNA) that is coincident with DNA. Thus, a portion of the protein in the DNA-PKcs–Ku complex is positioned directly over the DNA, and we cannot exclude the possibility that the DNA passes directly through the protein structure. The appearance of these complexes was not influenced by DNA with different overhanging or blunt ends (Table 4).

*Effect of Autophosphorylation on Protein–DNA Complexes.* We have previously shown that, in the presence of sonicated calf thymus DNA, purified DNA-PKcs, Ku70, and Ku80 undergo phosphorylation, and that phosphorylation

Table 3: Effect of ATP on Interaction of DNA-PKcs with Ku and DNA Ends<sup>a</sup>

reaction conditions	type of DNA end	no. of large protein-DNA complexes	protein complexes per DNA population	range of protein complexes per DNA population	no. of protein complexes containing multiple DNA molecules	average no. of Ku molecules per DNA population	range of Ku molecules per DNA population	average no. of residual DNA-PKcs molecules per DNA population	range of residual DNA-PKcs molecules per DNA population	<i>n</i>
-ATP	5' 4 bp overhangs	161	1.23	0-4	65 (50%)	1.06	0-5	0.15	0-2	131
+ATP	5' 4 bp overhangs	11	0.24	0-3	2 (6%)	1.39	0-6	0.17	0-2	46
-ATP	3' 4 bp overhangs	40	1.18	0-3	21 (62%)	1.74	0-5	0.18	0-2	34
+ATP	3' 4 bp overhangs	5	0.25	0-3	2 (10%)	1.45	0-6	0.15	0-1	20
-ATP	blunt	45	1.29	0-4	20 (57%)	1.60	0-4	0.14	0-1	35
+ATP	blunt	4	0.20	0-3	1 (5%)	1.35	0-5	0.20	0-2	20

<sup>a</sup> Ku70/80 and DNA-PKcs were incubated with various forms of linear DNA (as indicated) alone or in the presence of ATP. The concentration of DNA in each sample was 5 nM. Ku and DNA-PKcs were present at 3 nM (equimolar amounts of each subunit). The number and size of protein complexes on each DNA molecule were determined. Large complexes were distinguishable from DNA-PKcs alone and Ku alone by size (see text for details). *n* indicates the number of DNA populations analyzed. For samples containing Ku or DNA-PKcs, this represents 1 molecule of DNA. For samples containing DNA-PKcs, Ku, and DNA, where multiple molecules of DNA were associated with multiple protein-DNA complexes, each individual large protein-DNA cluster was counted as one population of DNA. The number of complexes observed relative to the total number of DNA molecules detected is shown in parentheses.

correlates with loss of protein kinase activity (21). Recently, it was suggested that linear plasmid dsDNA does not support either autophosphorylation or inactivation of DNA-PK (30). Before examining the effects of autophosphorylation on the formation of DNA-PK-DNA complexes, we first examined the ability of various linear dsDNA molecules to support both autophosphorylation and loss of DNA-PK protein kinase activity. Highly purified DNA-PKcs and Ku were incubated under autophosphorylation conditions with either sonicated calf thymus DNA or linearized plasmid dsDNA, and the incorporation of phosphate into DNA-PKcs, Ku70, and Ku80 was compared. The effect of the various DNA molecules on DNA-PK protein kinase activity was determined as described previously (21, 22). Linearized plasmid dsDNA (LIN-DNA) (Figure 3A) and M13 single-stranded closed circular DNA (data not shown) both supported phosphorylation of DNA-PKcs at a rate similar to that observed using sonicated calf thymus DNA (CT-DNA). Similar results were observed for phosphorylation of Ku70 and Ku80 (data not shown). As shown in Figure 3B, linear plasmid dsDNA and sonicated calf thymus DNA both supported loss of DNA-PK protein kinase activity. These autophosphorylation experiments were carried out using 10  $\mu$ g/mL linearized plasmid dsDNA, which corresponds to the DNA concentrations used in the ESI experiments. Similar results were obtained with a range of DNA concentrations (data not shown).

Having determined that linear plasmid dsDNA was capable of supporting both autophosphorylation and loss of protein kinase activity, we next determined the effect of preincubation of DNA-PKcs and Ku with linear dsDNA in the presence of Mg-ATP. In mock reactions, DNA-PKcs and Ku were preincubated with MgCl<sub>2</sub> alone. In the absence of ATP, most of the DNA and protein was present in large protein-DNA complexes with multiple DNA loops, as observed previously. Approximately 50–60% of the large protein-DNA complexes contained multiple DNA molecules, and, on average, the protein-DNA clusters had approximately one large protein complex bound to each DNA population (Table 3).

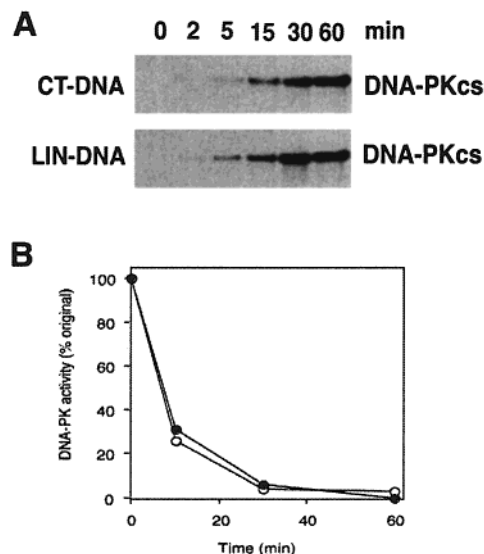


FIGURE 3: Linearized plasmid dsDNA supports phosphorylation and inactivation of DNA-PK: 210 ng of DNA-PKcs and 70 ng of Ku70/80 were incubated under standard autophosphorylation conditions with either sonicated calf thymus DNA (CT-DNA) or linearized plasmid dsDNA (LIN-DNA), both at 10 ng/mL. Aliquots were removed at the times indicated and either analyzed by SDS-PAGE, followed by autoradiography (panel A), or assayed for DNA-PK protein kinase activity in standard DNA-PK assays containing the synthetic peptide substrate (PESQEAFLWKK), with either CT-DNA (open circles) or LIN-DNA (closed circles) at 10 ng/mL (panel B).

When DNA-PKcs and Ku were incubated under conditions that support protein autophosphorylation (Figure 3A), a dramatic reduction in the number of large protein-DNA complexes was observed (Table 3 and Figure 4A). Under these conditions, the average number of large protein complexes per DNA population decreased by about 80% (Table 3), and the percentage of protein complexes containing multiple DNA molecules was reduced from 50–60% to under 10% (Table 3). Again these results were not affected by the presence of DNA with different ends. Autophospho-

Table 4: Effect of Wortmannin, AMP-PNP, and Protein Phosphatase 1 on the Interaction of DNA-PKcs and Ku with DNA<sup>a</sup>

reaction conditions	no. of large protein–DNA complexes	no. of protein complexes per DNA population	range of protein complexes per DNA population	no. of protein complexes containing multiple DNA molecules	average no. of Ku molecules per DNA population	range of Ku molecules per DNA population	average no. of DNA-PKcs molecules per DNA population	range of DNA-PKcs molecules per DNA population	<i>n</i>
+ATP+WM	17	1.13	0–3	10 (63%)	1.13	0–5	0.19	0–1	16
+AMP-PNP	17	1.06	0–4	9 (60%)	1.07	0–3	0.20	0–1	15
+ATP+PP1	43	1.43	0–4	27 (90%)	0.97	0–4	0.17	0–1	30
+ATP+[PP1+MC]	8	0.27	0–2	2 (7%)	1.00	0–4	0.23	0–2	30

<sup>a</sup> Ku70/80 and DNA-PKcs were incubated with linear dsDNA alone (–ATP) or in the presence of ATP or AMP-PNP, as indicated. Where indicated, wortmannin (WM) was added to DNA-PKcs prior to addition to the DNA-binding reaction. Samples containing the protein phosphatase 1 catalytic subunit (PP1) or inactive PP1 [PP1+MC], that had been incubated with Microcystin-LR, were added after the phosphorylation reaction. All measurements were as described in Table 3.

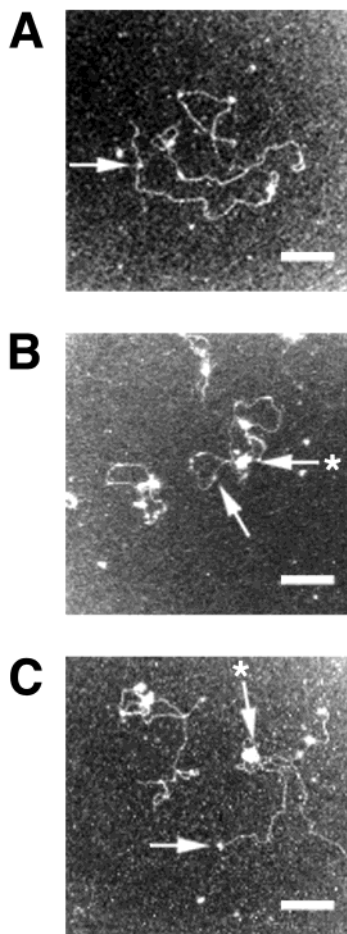


FIGURE 4: Phosphorylation results in disruption of DNA-PK–DNA protein complexes. Panel A: DNA-PKcs, Ku70/80, and DNA were incubated in the presence of 5 mM MgCl<sub>2</sub> plus 0.5 mM ATP for 60 min, and then prepared for microscopy. The arrow indicates an example of DNA-bound Ku. Panel B: As in panel A, but wortmannin (final concentration 1 μM) was added to reactions before the addition of Mg-ATP. The arrow with the asterisk indicates large protein–DNA complexes. The plain arrow indicates DNA-bound Ku. Panel C: As in panel A, but DNA-PKcs, Ku, and DNA were incubated with the nonhydrolyzable ATP analogue AMP-PNP (0.5 mM) instead of ATP. The plain arrow and the arrow with the asterisk indicate DNA-bound Ku and large DNA-PKcs–Ku–DNA complexes, respectively. The scale bars in panels A, B, and C represent 100 nm.

rylation also resulted in an increase in the proportion of DNA molecules that contained Ku alone (see, for example, Figure 4A); however, the number of DNA-PKcs molecules bound to DNA ends remained approximately constant (Table 3).

These data provide compelling evidence that phosphorylation disrupts the DNA-PK–DNA complexes, both reducing the number of complex protein–DNA structures and reducing the amount of DNA associated with each protein structure.

DNA-PK protein kinase activity is inhibited by the fungal metabolite wortmannin (8, 14, 16), which binds to the ATP-binding site of DNA-PKcs and other phosphatidylinositol 3-kinase-like enzymes (31). Wortmannin prevents autophosphorylation of DNA-PKcs and Ku (32), and would therefore be expected to prevent DNA-PK from undergoing autophosphorylation-induced loss of protein kinase activity. When DNA-PK was incubated with wortmannin (1 μM) prior to autophosphorylation, large protein–DNA complexes were observed at a frequency comparable to those seen in samples created in the absence of ATP. Under these conditions, the average number of large protein complexes per DNA population was approximately 1, and the percentage of protein complexes containing multiple DNA molecules increased from 6% (+ATP) (Table 3) to over 60% (+ATP+WM) (Table 4). The protein–DNA complexes observed had a similar appearance to those observed in the absence of ATP (Figure 4B). Thus, inactivating the protein kinase activity of DNA-PK with wortmannin virtually abolished the effects of phosphorylation on the DNA-PK–DNA complexes.

We previously showed that incubation of DNA-PK in the presence of the nonhydrolyzable ATP analogue AMP-PNP did not result in loss of DNA-PK kinase activity, consistent with ATP hydrolysis being required for phosphorylation and hence inactivation of DNA-PK (21). Thus, we would predict that incubation of DNA-PKcs and Ku with DNA in the presence of AMP-PNP would not lead to disruption of large protein complexes. Using ESI, we show that this was indeed the case (Table 4). Both the number of DNA molecules that were associated with large protein–DNA complexes and the total number of large protein complexes were close to those observed in the absence of ATP. Also, the appearance of the large protein–DNA complexes observed in the presence of AMP-PNP was similar to that observed in the absence of ATP (Figure 4C). These data support our hypothesis that autophosphorylation disrupts the DNA-PK–DNA complex.

*Protein Phosphatase Treatment Reverses the Effects of Mg-ATP on DNA-PK Complex Formation.* We have recently shown that protein phosphatases can remove phosphate groups from autophosphorylated DNA-PKcs, Ku70, and Ku80, and restore protein kinase activity in vitro (22). To determine if protein phosphatase treatment was able to restore

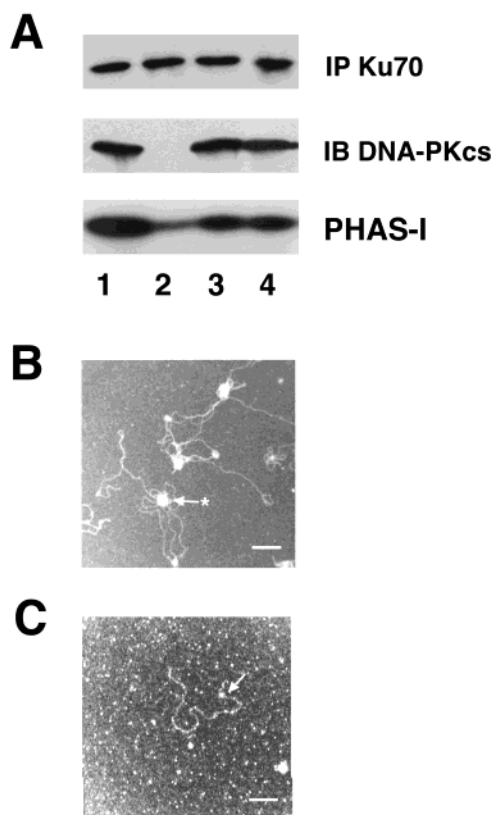


**FIGURE 5:** Protein phosphatase treatment reverses the effects of autophosphorylation on the DNA-PK–DNA complex. Panel A: DNA-PKcs, Ku, and DNA were incubated under identical conditions to those in Figure 4. The sample in lane 1 contained no ATP. The sample in lane 2 was incubated in the presence of ATP (0.5 mM) for 60 min. The sample in lane 3 was incubated with ATP for 60 min, followed by addition of PP1 (40 milliunits/mL) and incubation for a further 5 min, and the sample in lane 4 was incubated with AMP-PNP (0.5 mM) for 60 min. An antibody to Ku70 was then used to immunoprecipitate the DNA-PK complex. Half of the immunoprecipitate was analyzed on SDS–PAGE followed by immunoblot for Ku70 or DNA-PKcs (panel A, upper and middle panels, respectively). The other half of the sample was incubated with  $[\gamma\text{-}^{32}\text{P}]\text{ATP}$  and PHAS-I (0.5  $\mu\text{g}$ ) in the presence of magnesium and DNA for 5 min. The reaction products were separated by SDS–PAGE, and PHAS-I phosphorylation was visualized by autoradiography (part A, lower panel). Panel B: DNA-PKcs, Ku, and DNA were incubated with Mg-ATP followed by PP1 exactly as for lane 3 in panel A, and analyzed by ESI microscopy. The arrow with an asterisk indicates a large DNA-PKcs–Ku complex. Panel C: As in panel B, but microcystin-LR (1  $\mu\text{M}$ ) was added to PP1 prior to addition to the autophosphorylation reaction. The arrow indicates Ku bound to DNA. The scale bars represent 100 nm.

formation of DNA-PK–DNA complexes, we incubated DNA-PKcs and Ku heterodimer with linear dsDNA in the absence of ATP (Figure 5A, lane 1), in the presence of Mg-ATP (Figure 5A, lane 2), in the presence of Mg-ATP followed by addition of protein phosphatase 1 (Figure 5A, lane 3), or in the presence of the nonhydrolyzable analogue of ATP, Mg-AMP-PNP (Figure 5A, lane 4). In each case, antibodies to Ku70/80 were used to immunoprecipitate the DNA-PK complex, and half of the immunoprecipitate was assayed for protein kinase activity using PHAS-I as substrate (shown in the lower panel of Figure 5A). The other half of the immunoprecipitate was transferred to nitrocellulose and probed with antibodies to Ku70 or DNA-PKcs as indicated (shown in the upper and middle panels of Figure 5A). As

expected, autophosphorylation resulted in loss of protein kinase activity and disruption of the DNA-PK–DNA complex (Figure 5A, lane 2). However, when protein phosphatase (PP1) was added to the reaction after autophosphorylation, the loss of protein kinase activity was reversed, and DNA-PKcs again immunoprecipitated with Ku (Figure 5A, lane 3). As predicted, incubation with Mg-AMP-PNP instead of Mg-ATP did not affect DNA-PK protein kinase activity or the ability of DNA-PKcs to interact with Ku (Figure 5A, lane 4). When we analyzed reactions that had been incubated under conditions that promote autophosphorylation followed by incubation with PP1, we observed a high percentage of large protein–DNA complexes containing multiple DNA loops. In a typical experiment, 43 large complexes were detected on 30 DNA molecules, representing 1.4 large protein complexes per DNA population. In addition, 90% of the large protein–DNA complexes contained multiple DNA molecules (Table 4). When autophosphorylated DNA-PK was preincubated with PP1 that had been inactivated by prior incubation with microcystin-LR, the number of large protein–DNA complexes observed was significantly reduced. In this experiment, 8 large complexes were detected on 30 DNA molecules, giving an average of 0.3 large complex per DNA population (Table 4). In addition, the number of large protein complexes that contained multiple DNA molecules was reduced to 7%, which was similar to that observed in autophosphorylation reactions (Table 4). Together, our results provide strong evidence that assembly and/or stability of the DNA-PK–Ku–DNA complex is regulated by reversible protein phosphorylation.

## DISCUSSION

Various imaging techniques have been used to study the interaction of Ku with DNA (5–7, 23); the interaction of DNA-PKcs with DNA-bound Ku, however, has been less well studied. Some imaging techniques used to date have involved rotary shadowing with heavy metals (5), or the use of the chemical cross-linker glutaraldehyde (6). In contrast, ESI can be performed without the need for either heavy atoms or glutaraldehyde treatment, and has the additional advantage that it can distinguish between protein and DNA within the same complex (24). Here, we have used ESI to examine the interaction of DNA-PKcs and Ku with DNA.

As observed in previous studies (6, 7), we find that the Ku heterodimer binds to linear dsDNA at ends and at internal sites, and that DNA-PKcs binds to ends of linear dsDNA. We show that when highly purified DNA-PKcs is incubated with Ku and linear plasmid dsDNA, the DNA undergoes a remarkable transformation from a linear molecule to a highly convoluted form, containing large protein complexes that are centered at the convergence of multiple DNA loops. The ratio of protein to DNA in the large complexes and the number of DNA strands observed in the large complexes suggest that the DNA-PK complex brings several DNA molecules together. Such behavior is consistent with the proposed role of DNA-PK in the detection and repair of DNA double-strand breaks. The multiple loops of DNA appeared to radiate from a central region of the DNA, with the protein molecule (shown in green and yellow in Figure 2F) situated at the convergence of the DNA loops. The yellow coloration in Figure 2F indicates convergence of protein and DNA, suggesting that the DNA and protein are in direct contact

and that either the protein is situated on top of the DNA loops or the DNA is threaded through the protein molecule.

Our findings raise several questions regarding the nature of the complexes that are observed in the presence of DNA-PKcs, Ku, and DNA. Several pieces of data suggest that the observed complexes are not due to nonspecific interactions between DNA-PKcs, Ku, and DNA. For example, the large complexes with multiple DNA loops were not observed with DNA alone, with DNA plus Ku, with DNA plus purified DNA-PKcs (Figures 1 and 2), or with DNA with BSA (data not shown). It is therefore interesting to speculate whether such complexes are formed during NHEJ, and, if so, how such multiple DNA-ends would be processed by the DNA double-strand break repair protein machinery. It is possible that when a DNA double-strand break occurs in the nucleus, the structural constraints of the chromatin prevent more than two ends of DNA from being accommodated within the repair complex. Alternatively, we speculate that other proteins involved in the repair process such as XRCC4, DNA ligase IV (1), Artemis (33, 34), or polynucleotide kinase (35), or factors such as inositol hexaphosphate (13, 36), could suppress the interaction of DNA-PK with multiple DNA ends and favor end-to-end rejoining of two pieces of DNA. Experiments to test this hypothesis are in progress. It is interesting to note that the product of the breast cancer susceptibility gene, BRCA1, also interacts with linear plasmid dsDNA molecules to form a protein–DNA complex in which BRCA1 is situated at the convergence of multiple DNA loops (37) and therefore resembles the complexes formed by DNA-PK and DNA.

The structure of the Ku70/80 dimer bound to DNA was recently solved to 2.5 Å, and revealed a relatively globular molecule of 12 nm × 7 nm × 6 nm, that does not undergo a significant change in size or shape upon binding to DNA (38). Using ESI, we estimated the size of the Ku heterodimer to be approximately 13 nm × 15 nm, which corresponds well with that determined by X-ray crystallography. Cryo-electron microscopy analysis of DNA-PKcs has revealed an open cage-like structure that is approximately spherical in shape, and has overall dimensions of 12 nm × 13 nm × 16 nm (39, 40). The size of DNA-PKcs bound to DNA as measured by ESI was approximately 30 nm × 26 nm. Since this is significantly larger than the size of an individual molecule of DNA-PKcs as determined by cryo-EM, we speculate that more than one molecule of DNA-PKcs may be present at the ends of DNA. Indeed, it has been suggested that DNA-PKcs binds to ends of DNA as a dimer (41), which is in good agreement with the dimensions determined from the line scan intensities of the ESI images. Also, a very recent study (42) has shown, using electron microscopy, that two molecules of DNA-end-bound DNA-PKcs indeed interact and bring two molecules of DNA together. This property of DNA-PK could be directly relevant to its role in nonhomologous end-joining, specifically, binding to DNA ends and bringing opposing DNA ends into a complex for subsequent ligation by XRCC4 and DNA ligase IV.

Using co-immunoprecipitation, we previously showed that DNA-PKcs and Ku interact in the presence of DNA, but that addition of Mg-ATP disrupted this interaction (21). Although these data were consistent with the possibility that autophosphorylation disrupted the interaction between DNA-PKcs and Ku, it was possible that binding of the antibody

to one protein could have affected its ability to interact with its partner protein. Here, using ESI, we provide direct evidence that conditions that promote autophosphorylation also promote disruption of the DNA-PKcs–Ku–DNA complex. Together, these data make a compelling case for autophosphorylation providing a mechanism to regulate the properties of DNA-PK at the site of the DNA double-strand break. We propose that DNA-PK assembles at the DNA double-strand break, and that autophosphorylation could serve to remove DNA-PKcs from the complex prior to ligation. We recently identified six *in vitro* autophosphorylation sites in DNA-PKcs (32). Interestingly, 5 phosphorylation sites occur in a stretch of 38 amino acids that is located in the central region of the protein. It is possible that autophosphorylation at this cluster of sites could induce a conformational change in DNA-PKcs that could influence its interaction with DNA-bound Ku, and perhaps account for the autophosphorylation-induced disruption of the DNA-PK–DNA complex observed here. Experiments to test this hypothesis are currently underway.

## ACKNOWLEDGMENT

We thank Dr. W. Michael Schoel for assistance in image and software analysis, and the University of Calgary Imaging Facility for assistance with microscopy. We also thank members of the Lees-Miller laboratory for helpful comments and critical reading of the manuscript.

## REFERENCES

- Norbury, C. J., and Hickson, I. D. (2001) *Annu. Rev. Pharmacol. Toxicol.* 41, 367–401.
- Pierce, A. J., Stark, J. M., Araujo, F. D., Moynahan, M. E., Berwick, M., and Jasin, M. (2001) *Trends Cell Biol.* 11, S52–59.
- Smith, G. C., and Jackson, S. P. (1999) *Genes Dev.* 13, 916–934.
- Blier, P. R., Griffith, A. J., Craft, J., and Hardin, J. A. (1993) *J. Biol. Chem.* 268, 7594–7601.
- de Vries, E., van Driel, W., Bergsma, W. G., Arnberg, A. C., and van der Vliet, P. C. (1989) *J. Mol. Biol.* 208, 65–78.
- Cary, R. B., Peterson, S. R., Wang, J., Bear, D. G., Bradbury, E. M., and Chen, D. J. (1997) *Proc. Natl. Acad. Sci. U.S.A.* 94, 4267–4272.
- Yaneva, M., Kowalewski, T., and Lieber, M. R. (1997) *EMBO J.* 16, 5098–5112.
- Gottlieb, T. M., and Jackson, S. P. (1993) *Cell* 72, 131–142.
- Lees-Miller, S. P., Godbout, R., Chan, D. W., Weinfeld, M., Day, R. S., III, Barron, G. M., and Allalunis-Turner, J. (1995) *Science* 267, 1183–1185.
- Chan, D. W., Mody, C. H., Ting, N. S., and Lees-Miller, S. P. (1996) *Biochem. Cell Biol.* 74, 67–73.
- Chen, S., Inamdar, K. V., Pfeiffer, P., Feldmann, E., Hannah, M. F., Yu, Y., Lee, J. W., Zhou, T., Lees-Miller, S. P., and Povirk, L. F. (2001) *J. Biol. Chem.* 276, 24323–24330.
- Baumann, P., and West, S. C. (1998) *Proc. Natl. Acad. Sci. U.S.A.* 95, 14066–14070.
- Hanakahi, L. A., Bartlett-Jones, M., Chappell, C., Pappin, D., and West, S. C. (2000) *Cell* 102, 721–729.
- Sarkaria, J. N., Tibbetts, R. S., Busby, E. C., Kennedy, A. P., Hill, D. E., and Abraham, R. T. (1998) *Cancer Res.* 58, 4375–4382.
- Hartley, K. O., Gell, D., Smith, G. C., Zhang, H., Divecha, N., Connelly, M. A., Admon, A., Lees-Miller, S. P., Anderson, C. W., and Jackson, S. P. (1995) *Cell* 82, 849–856.
- Izzard, R. A., Jackson, S. P., and Smith, G. C. (1999) *Cancer Res.* 59, 2581–2586.
- Boulton, S., Kyle, S., and Durkacz, B. W. (2000) *Eur. J. Cancer* 36, 535–541.
- Chernikova, S. B., Wells, R. L., and Elkind, M. M. (1999) *Radiat. Res.* 151, 159–166.

19. Kurimasa, A., Kumano, S., Boubnov, N. V., Story, M. D., Tung, C. S., Peterson, S. R., and Chen, D. J. (1999) *Mol. Cell. Biol.* **19**, 3877–3884.
20. Lees-Miller, S. P., Chen, Y. R., and Anderson, C. W. (1990) *Mol. Cell. Biol.* **10**, 6472–6481.
21. Chan, D. W., and Lees-Miller, S. P. (1996) *J. Biol. Chem.* **271**, 8936–8941.
22. Douglas, P., Moorhead, G. B. G., Ye, R., and Lees-Miller, S. P. (2001) *J. Biol. Chem.* **276**, 18992–18998.
23. Pang, D., Yoo, S., Dynan, W. S., Jung, M., and Dritschilo, A. (1997) *Cancer Res.* **57**, 1412–1415.
24. Bazett-Jones, D. P., and Hendzel, M. J. (1999) *Methods: Compan. Methods Enzymol.* **17**, 188–200.
25. Bazett-Jones, D. P., Cote, J., Landel, C. C., Peterson, C. L., and Workman, J. L. (1999) *Mol. Cell. Biol.* **19**, 1470–1478.
26. Bazett-Jones, D., Kimura, K., and Hirano, T. (2002) *Mol. Cell* **9**, 1183–1190.
27. Paillard, S., and Strauss, F. (1991) *Nucleic Acids Res.* **19**, 5619–5624.
28. Ting, N. S., Kao, P. N., Chan, D. W., Lintott, L. G., and Lees-Miller, S. P. (1998) *J. Biol. Chem.* **273**, 2136–2145.
29. Stefanovsky, V. Y., Pelletier, G., Bazett-Jones, D. P., Crane-Robinson, C., and Moss, T. (2001) *Nucleic Acids Res.* **29**, 3241–3247.
30. Soubeyrand, S., Torrance, H., Giffin, W., Gong, W., Schild-Poulter, C., and Hache, R. J. (2001) *Proc. Natl. Acad. Sci. U.S.A.* **98**, 9605–9610.
31. Wymann, M. P., Bulgarelli-Leva, G., Zvelebil, M. J., Pirola, L., Vanhaesebroeck, B., Waterfield, M. D., and Panayotou, G. (1996) *Mol. Cell. Biol.* **16**, 1722–1733.
32. Douglas, P., Sapkota, G. P., Morrice, N., Yu, Y., Goodarzi, A. A., Merkle, D., Meek, K., Alessi, D. R., and Lees-Miller, S. P. (2002) *Biochem. J.* (Aug 19 epub).
33. Moshous, D., Callebaut, I., de Chasseval, R., Corneo, B., Cavazana-Calvo, M., Le Deist, F., Tezcan, I., Sanal, O., Bertrand, Y., Philippe, N., Fischer, A., and de Villartay, J. P. (2001) *Cell* **105**, 177–186.
34. Ma, Y., Pannicke, U., Schwarz, K., and Lieber, M. R. (2002) *Cell* **108**, 781–794.
35. Chappell, C., Hanakahi, L. A., Karimi-Busheri, F., Weinfeld, M., and West, S. C. (2002) *EMBO J.* **21**, 2827–2832.
36. Hanakahi, L. A., and West, S. C. (2002) *EMBO J.* **21**, 2038–2044.
37. Paull, T. T., Cortez, D., Bowers, B., Elledge, S. J., and Gellert, M. (2001) *Proc. Natl. Acad. Sci. U.S.A.* **98**, 6086–6091.
38. Walker, J. R., Corpina, R. A., and Goldberg, J. (2001) *Nature* **412**, 607–614.
39. Chiu, C. Y., Cary, R. B., Chen, D. J., Peterson, S. R., and Stewart, P. L. (1998) *J. Mol. Biol.* **284**, 1075–1081.
40. Leuther, K. K., Hammarsten, O., Kornberg, R. D., and Chu, G. (1999) *EMBO J.* **18**, 1114–1123.
41. Hammarsten, O., DeFazio, L. G., and Chu, G. (2000) *J. Biol. Chem.* **275**, 1541–50.
42. DeFazio, L. G., Stansel, R. M., Griffith, J. D., and Chu, G. (2002) *EMBO J.* **21**, 3192–3200.

BI0263558